Determination of the Nucleotide Binding Site within *Clostridium symbiosum* Pyruvate Phosphate Dikinase by Photoaffinity Labeling, Site-Directed Mutagenesis, and Structural Analysis†

Marielena McGuire, Lawrence J. Carroll, Linda Yankie, Sara H. Thrall, and Debra Dunaway-Mariano*

Department of Chemistry and Biochemistry, University of Maryland, College Park, Maryland 20742

Osnat Herzberg

Center for Applied Research and Biotechnology, University of Maryland Biotechnology Institute, 9600 Gudelsky Drive, Rockville, Maryland 20850

Beby Jayaram and Boyd H. Haley

Markey Cancer Center, University of Kentucky, Lexington, Kentucky 40536

Received February 5, 1996; Revised Manuscript Received March 29, 1996⊗

ABSTRACT: *Clostridium symbiosum* pyruvate phosphate dikinase (PPDK) catalyzes the interconversion of adenosine 5′-triphosphate (ATP), orthophosphate (P_i), and pyruvate with adenosine 5′-monophosphate (AMP), pyrophosphate (PP_i), and phosphoenolpyruvate (PEP). The nucleotide binding site of this enzyme was labeled using the photoaffinity reagent [^{32}P]-8-azidoadenosine 5′-triphosphate ([^{32}P]-8-azidoATP). Subtilisin cleavage of the [α-^{32}P]-8-azidoATP-photolabeled PPDK into domain-sized fragments, prior to SDS−PAGE analysis, allowed us to identify two sites of modification: one between residues 1 and 226 and the other between residues 227 and 334. Saturation of the ATP binding site with adenylyl imidodiphosphate afforded protection against photolabeling. Next, small peptide fragments of [γ-^{32}P]-8-azidoATP-photolabeled PPDK were generated by treating the denatured protein with trypsin or α-chymotrypsin. A pair of overlapping radiolabeled peptide fragments were separated from the two digests, DMQDMEFTIEEGK (positions 318−330 in trypsin-treated PPDK) and RDMQDMEFTIEEGKL (positions 317−331 in α-chymotrypsin-treated PPDK), thus locating one of the positions of covalent modification. Next, catalysis by site-directed mutants generated by amino acid replacement of invariant residues of the PPDK N-terminal domain was tested. K163L, D168A, D170A, D175A, K177L, and G248I PPDK mutants retained substantial catalytic activity while G254I, R337L, and E323L PPDK mutants were inhibited. Comparison of the steady-state kinetic constants measured (at pH 6.8, 25 °C) for wild-type PPDK (k_{cat} = 36 s^{-1}, $^{AMP}K_m$ = 7 μM, $^{PP_i}K_m$ = 70 μM, $^{PEP}K_m$ = 27 μM) to those of R337L PPDK (k_{cat} = 2 s^{-1}, $^{AMP}K_m$ = 85 μM, $^{PP_i}K_m$ = 3700 μM, $^{PEP}K_m$ = 6 μM) and G254I PPDK (k_{cat} = 0.1 s^{-1}, $^{AMP}K_m$ = 1300 μM, $^{PP_i}K_m$ = 1200 μM, $^{PEP}K_m$ = 12 μM) indicated impaired catalysis of the nucleotide partial reaction (E·ATP·P_i → E−PP·AMP·P_i → E−P·AMP·PP_i) in these mutants. The single turnover reactions of [^{32}P]PEP to [^{32}P]E−P·pyruvate catalyzed by the PPDK mutants were shown to be comparable to those of wild-type PPDK. In contrast, the formation of [^{32}P]E−PP/[^{32}P]E−P in single turnover reactions of [β-^{32}P]ATP/P_i was significantly inhibited. Finally, the location of the adenosine 5′-diphosphate binding site within the nucleotide binding domain of D-alanine−D-alanine ligase, a structural homologue of the PPDK N-terminal domain [Herzberg, O. (1996) *Proc. Natl. Acad. Sci. U.S.A. 93,* 2652−2657] indicates, by analogy, the location of the nucleotide binding site in PPDK. Residues G254, R337, and E323 as well as the site of photoaffinity labeling are located within this region.

Pyruvate phosphate dikinase (PPDK)[1] catalyzes the interconversion of ATP, P_i, and pyruvate with AMP, PP_i, and PEP in certain microorganisms and plants [for review see Wood et al. (1977) and Cooper and Kornberg (1974)]. The structure and mechanism of action of this enzyme are quite remarkable. Catalysis (in the PEP-forming reaction) involves the transfer of the ATP γ-phosphoryl group to P_i and the β-phosphoryl group to pyruvate (Reeves et al., 1968). As illustrated in Scheme 1, these two phosphoryl transfers are mediated by an active site histidine which first displaces AMP from the β-phosphoryl of ATP forming a pyrophosphorylated enzyme intermediate (Spronk et al., 1976). Phosphoryl transfer occurs from the pyrophosphorylhistidine residue to P_i and then from the resulting phosphorylhistidine residue to pyruvate (Carroll et al., 1989, 1990; Thrall et al., 1993). Transient kinetic studies of PPDK catalysis indicate that the nucleotide partial reaction (steps 1 and 2 of Scheme 1) and the pyruvate partial reaction (step 3, Scheme 1) occur at separate active sites (Thrall & Dunaway-Mariano, 1994).

† This work was supported by NIH Grant GM-36260 to D.D.-M., NSF Grant MCB 9316934 to O.H., and NIH Grant GM-35766 to B.H.H.

* Corresponding author.

⊗ Abstract published in *Advance ACS Abstracts,* June 15, 1996.

S0006-2960(96)00275-9 CCC: $12.00

Scheme 1: Chemical Steps of PPDK Catalysis[a]

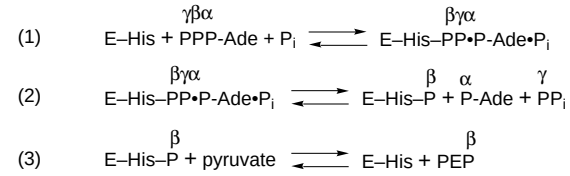

[a] Wood et al., 1977; Carroll et al., 1989, 1990; Thrall et al., 1993. E, E−P, and E−PP represent the free enzyme, phosphoryl enzyme, and pyrophosphoryl enzyme, respectively.

The X-ray crystallographic structure of apoPPDK from *Clostridium symbiosum* reveals that the 96 kDa enzyme is organized into three consecutive structural domains (Herzberg et al., 1996). As illustrated in Figure 1, these include an N-terminal domain (colored green) spanning residues 1−340, connected by a helical linker (residues 341−389; red) to a central domain (residues 390−504; yellow) which in turn is connected by a helical linker (residues 505−533; red) to the C-terminal domain (residues 554−874; blue). The catalytic residue His455 resides on the central domain while the PEP/pyruvate binding site is located on the C-terminal domain (Carroll et al., 1994; Xu et al., 1995a,b; Yankie et al., 1995).

In an earlier study we showed that the lysine-directed affinity label [^{14}C]oAMP covalently modifies a residue contained within the first 226 residues of the protein (Carroll et al., 1994). The protection afforded by AMP demonstrated that the site of modification is in or nearby the nucleotide binding site. However, despite the numerous attempts made, we were unable to identify which PPDK lysine residue was labeled by the [^{14}C]oAMP (Thrall, 1993). The radiolabel proved to be too unstable for recovery from proteolytic digests of the modified protein. In the present study, the photoaffinity reagent [^{32}P]-8-azidoATP was used to label the nucleotide binding site. In parallel, site-directed mutagenesis of invariant amino acid residues was carried out to identify those residues required for nucleotide binding/catalysis. Finally, the overall fold of the PPDK N-terminal domain (Herzberg et al., 1996) was compared with that of D-alanine−D-alanine ligase (Fan et al., 1994, 1995) to arrive at an assignment for the nucleotide binding site.

MATERIALS AND METHODS

Materials. PPDK (*C. symbiosum*) was purified to homogeneity from *Escherichia coli* JM101 cells transformed with the PPDK-encoding recombinant plasmid pACYC184 D12 (Pocalyko et al., 1990) by using the purification procedure described by Wang et al. (1988). [^{32}P]PEP and [β-^{32}P]ATP were prepared from commercial [γ-^{32}P]ATP (NEN) according to the method of Carroll et al. (1989). [α-^{32}P]-8-AzidoATP (SA = 1 mCi/μmol) was purchased from ICN.

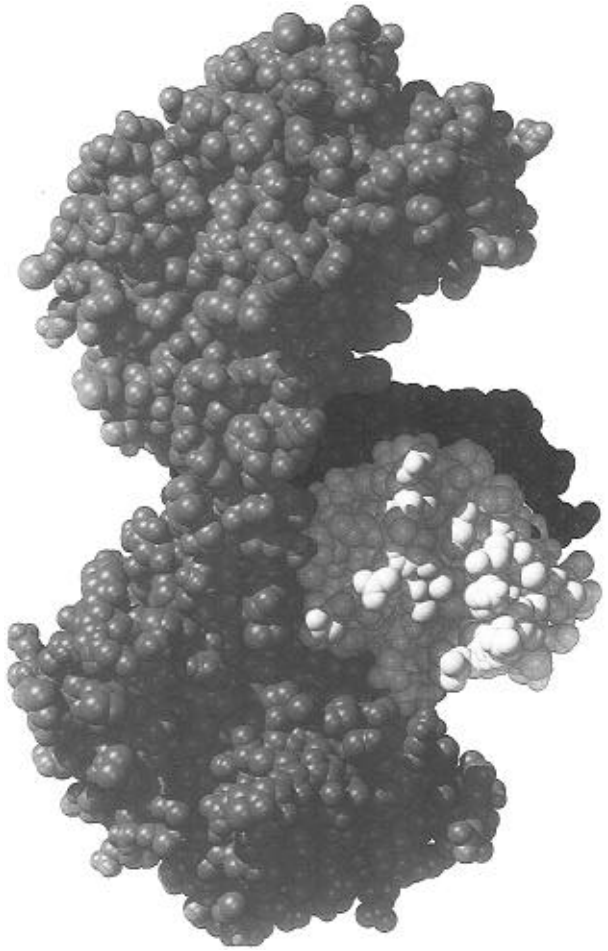

FIGURE 1: Space-filling representation of the X-ray crystal structure of *C. symbiosum* apoPPDK determined at 2.3 Å resolution (Protein Data Bank entry code 1DIK). Atoms of the N-terminal domain (residues 1−340) are shown as green spheres. Those of the phosphohistidine domain (residues 390−504) are shown as yellow spheres and those of the C-terminal domain as blue spheres (residues 554−874). The two interdomain helical linkers (residues 341−389 and residues 505−533) are shown in red.

[γ-^{32}P]-8-AzidoATP (SA = 10−20 mCi/μmol) was prepared from 8-azidoATP and [^{32}P]H_3PO_4 (ICN) by using the exchange reaction method described previously (Potter et al., 1983; Czarnecki et al., 1979). The immobilized Al^{3+} affinity column was prepared by washing 1 mL of iminodiacetic acid−epoxy-activated Sepharose 63 fast flow resin (Sigma) contained in a 15 mL conical plastic tube successively (3 × 10 mL each) with H_2O, 50 mM $AlCl_3$, H_2O, 100 mM ammonium acetate (pH 6.0), 100 mM ammonium acetate (pH 6.0)/0.5 M KCl/2 M urea, and 100 mM ammonium acetate (pH 6.0) (Jayaram & Haley, 1994). All PCR reagents were from Perkin-Elmer.

Photoaffinity Labeling Experiments with [^{32}P]-8-AzidoATP. *(A) SDS−PAGE Analysis*. Solutions (200 μL) containing 10 μM PPDK, 50 μM [α-^{3}12P]-8-azidoATP, 5 mM $MgCl_2$, 10 mM NH_4Cl, 1 mM potassium phosphate, 50 mM K^+Hepes (pH 7), and 1 mM AMPPNP or adenosine as indicated were photolyzed at 23 °C for 1 min with a hand-held ultraviolet lamp (UVGL-25 Mineral lamp, 254 nm, 200 μW/cm^2). Reactions were quenched with 50 mM DTT. Subtilisin Carlsberg was added to a concentration of 0.05 μg/μL except for the sample containing AMPPNP where 0.2 μg/μL was used. After specified time periods 30 μL aliquots were removed, quenched by the addition of 2 μL of PMSF

[1] Abbreviations: PPDK, pyruvate phosphate dikinase; ATP, adenosine 5′-triphosphate; AMP, adenosine 5′-monophosphate; PEP, phosphoenolpyruvate; P_i, orthophosphate; PP_i, pyrophosphate; HPLC, high-performance liquid chromatography; Hepes, *N*-(2-hydroxyethyl)piperazine-*N*′-2-ethanesulfonic acid; SDS−PAGE, sodium dodecyl sulfate−polyacrylamide gel electrophoresis; E−P, phosphoryl enzyme; E−PP, pyrophosphoryl enzyme; oAMP, 2′,3′-dialdehyde adenosine 5′-monophosphate; EDTA, ethylenediaminetetraacetic acid; DTT, dithiothreitol; TFA, trifluoroacetic acid; TEA, triethylamine; EGTA, ethylene glycol bis(β-aminoethyl ether)-*N*,*N*,*N*′,*N*′-tetraacetic acid; 8-azidoATP, 8-azidoadenosine 5′-triphosphate; Pipes, piperazine-*N*,*N*′-bis(2-ethanesulfonic acid); Tris, tris(hydroxymethyl)aminomethane; AMPPNP, adenylyl imidodiphosphate; SA, specific activity; D-Ala-D-Ala ligase, D-alanine−D-alanine ligase.

(in DMF), mixed with gel loading buffer, and chromatographed at 25 mA on a 12% SDS−PAGE gel.

(B) Trypsin/Chymotrypsin Digestion and Peptide Sequencing. The concentration dependence of PPDK photolabeling with [γ-^{32}P]-8-azidoATP and protection by ATP was examined first to ensure that photolabeling was occurring at the ATP binding site. Plots of the incorporation of ^{32}P vs [γ-^{32}P]-8-azidoATP concentration or vs ATP concentration (at fixed [γ-^{32}P]-8-azidoATP concentration) are shown in Figure 1 of Supporting Information. For preparation of labeled protein, 2 mg of PPDK was incubated on ice in 0.5 mL of photolysis buffer (10 mM potassium phosphate, 200 μM $MgCl_2$, and 20 μM $ZnCl_2$ at pH 8) with a solution depth of about 3 mm. At 1 min 20 μM [γ-^{32}P]-8-azidoATP was added, and the resulting solution was incubated for 1 min. Photolysis was then carried out for 1 min, followed by a second incubation with fresh photoprobe for 1 min and subsequent photolysis for 1 min. The unreacted azide was reduced by quenching the reaction with 10 mM DTT. The modified protein was precipitated with 6% trichloroacetic acid and pelleted by centrifugation. The protein pellet was washed twice with ice-cold methanol, and the residual methanol was removed *in vacuo*. The protein residue was dissolved in 1 mL of buffer containing 100 mM ammonium bicarbonate, 2 M urea, and 5 mM each of DTT and iodoacetic acid (pH 8.0) and digested by three sequential additions of trypsin or α-chymotrypsin (8−10% w/w) for 10−12 h at 25 °C, as described in Stone et al. (1989). The resulting solution was diluted to 5 mL with 100 mM ammonium acetate (pH 6.0) and then loaded onto a 5 mL plastic column of Al^{3+} affinity resin (see Materials). The column was successively washed with 30 volumes each of 100 mM ammonium acetate (pH 6.0), 100 mM ammonium acetate (pH 6.0)/0.5 M KCl/2 M urea, and 100 mM ammonium acetate (pH 6.0). The column was then eluted with 20 mL of 20 mM potassium phosphate (pH 8.0). The 2 mL column fractions were assayed for radioactivity by scintillation counting. The radioactive fractions obtained with the phosphate buffer eluant were pooled, concentrated *in vacuo* to near dryness, and then diluted to 2 mL with 0.1% TFA. HPLC chromatography was carried out using an Aquapore RP-300, C8 column (250 × 4.66 mm, Browlee Laboratories) and an LB-HPLC system having a diode array spectral detector. The column was developed at 0.5 mL/min with a linear gradient of 70% acetronitrile in 0.1% TFA; from 0−5 min, 0.1% TFA; at 65 min, 70% acetonitrile in 0.1% TFA; and at 70 min, 0.1% TFA. One-half milliliter fractions were collected and analyzed for radioactivity by scintillation counting. The radioactive fractions were concentrated *in vacuo* to *ca*. 0.1 mL. Sequence analysis of these fractions was carried out using an Applied Biosystems 477A pulse liquid protein sequencer.

Construction, Purification, and Characterization of PPDK Site-Directed Mutants. Site-directed mutants were made using PCR techniques (Erlich, 1992) and a Thermolyne Temp·Tronic thermocycler. Primary PCR reactions contained 50 mM KCl, 10 mM Tris·HCl (pH 8.3), 200 μM each of dATP, dCTP, dGTP, and dTTP, 20 pM each primer, 2.5 units of Taq DNA polymerase, 1.5 mM $MgCl_2$, and 0.5 μg of template DNA (pACYC 184 D12; Pocalyko et al., 1990). First, a unique *Bgl*II restriction site (AGATATCT) was introduced at nucleotides 188−193 without altering the code. Mutant primers corresponded to nucleotides 186−206 in the wild-type PPDK gene. Outside primers corresponded to positions 1517−1531 in the pACYC 184 sequence (Chang & Cohen, 1978) and positions 998−1114 in the PPDK negative strand sequence (these positions are just upstream of the unique *Xba*I restriction site in pACYC 184 and downstream of the unique *Bst*XI restriction site in the PPDK gene). The primary PCR was conducted at 92 °C for 1 min, with annealing at 55 °C for 1 min and extension at 72 °C for 2 min. Each primary PCR reaction was cycled 25 times. For the secondary PCR 3 mM $MgCl_2$ and 1.0 μg of template were used. Following each PCR, the DNA was chromatographed on a 1% LP agarose gel with Tris (10.8 g/L)/boric acid (5.5 g/L)/EDTA (0.74 g/L) buffer and then extracted from the gel using the Gene Clean kit from Bio101. The 2.6 kb fragments and the wild-type pACYC 184 D12 were both digested with *Xba*I and *Bst*XI according to the manufacturer's recommended protocol. Following purification by gel electrophoresis the two fragments were ligated using T4 DNA ligase (37 °C, 4.5 h), and the resulting mutant plasmid was used to transform competent JM101 *E. coli* cells by the method described in Sambrook et al. (1989). The mutant was verified by DNA sequencing using the chain termination method (Sanger et al., 1977) and the Sequenase kit from United States Biologicals. The mutated plasmid pACYC 184 D12 *Bgl*II was used in conjunction with the protocol described above to construct each of the following site-directed mutants: K163L (AAG to CTG), D168A (GAT to GCC), D170A (GAC to GCG), D175A (GAT to GCG), KI77L (AAA to ACT), G248I (GGC to ATC), G254I (GGC to ATC), E323L (GAG to CTG), and R337L (CGT to CTA). The primers and restriction enzymes used in the construction of these mutants are provided in Table I of Supporting Information. The mutant plasmids were verified by DNA sequencing and expressed in JM101 *E. coli* cells. The mutant enzymes were purified and quantitated using the protocols described in Yankie et al. (1995). The specific activities of the purified mutant enzymes were determined using the spectrophotometric assay described in Wang et al. (1988) to measure pyruvate formation via reduction with NADH/lactate dehydrogenase. Assay solutions (1 mL, 25 °C) contained 0.5 mM AMP, 0.5 mM PEP, 1 mM PP_i, 40 mM NH_4Cl, 5 mM $MgCl_2$, 0.2 mM NADH, and 22 units of lactate dehydrogenase in 20 mM imidazole hydrochloride (pH 6.4). Reactions were initiated by the addition of the 1 mM PP_i and monitored by measuring the decrease in absorbance at 340 nm.

Steady-State Kinetic Analysis of G254I and R337L PPDK Mutants. The k_{cat} and K_m values for catalysis in the pyruvate-forming direction were measured using the spectrophotometric assay described above. For each substrate, the initial velocity of the catalyzed reaction was measured at varying substrate concentrations (within the range of $0.5K_m$ to $10K_m$) and at a fixed, saturating concentration of cosubstrate (1.0 mM PP_i, 0.5 mM PEP, 0.5 mM AMP). The initial velocity data were analyzed using eq 1 (in which V_0 is the initial

$$V_0 = V_m[S]/(K_m + [S]) \quad (1)$$

velocity of the reaction, V_m is the maximum velocity, K_m is the Michaelis constant, and [S] is the substrate concentration) and the HYPER data fitting program (Cleland, 1979) for a Macintosh computer. The k_{cat} values were calculated by dividing the V_m by the enzyme concentration used in the experiment (16.4 nM wild-type PPDK, 0.14 μM R337L PPDK, 14 μM G254I PPDK). The k_{cat} for catalysis in the

AMP-forming direction was measured using a fixed time assay in which [^{14}C]ATP was used in conjunction with HPLC separation of reactants and products (Mehl et al., 1994). Reaction solutions (80 μL) contained 2 mM [^{14}C]ATP, 5 mM pyruvate, 5 mM P_i, 20 units of inorganic pyrophosphatase, 5 mM $MgCl_2$, and 10 mM NH_4Cl. Reactions were initiated by the addition of 1 μM wild-type PPDK, 20 μM R337L PPDK, or 40 μM G254I PPDK. Reactions were quenched at varying conversions (5−90%) by the addition of 164 μL of 0.6 M HCl. The enzyme was precipitated by vortexing the reaction solution with 100 μL of CCl_4 and removed by centrifugation. The supernatant was neutralized with 5 M NaOH and chromatographed on a 4.6 mm × 25 cm reversed-phase Beckman ultrasphere C18 analytical HPLC column with 25 mM KH_2PO_4, 2.5% triethylamine, and 5% methanol (pH 4.2) at a flow rate of 1 mL/min. The chromatography was monitored at 260 nm, and the fractions corresponding to [^{14}C]ATP and [^{14}C]AMP were collected and analyzed by liquid scintillation counting. The initial velocity was determined from the reaction time courses ([AMP] vs time) and used as the estimated maximum velocity, from which k_{cat} was calculated.

Transient Kinetic Measurements of the Nucleotide and Pyruvate Partial Reactions Catalyzed by Wild-Type PPDK, G254I PPDK, and R337L PPDK. For each time point, a 40 μL solution containing 80 μM enzyme active sites, 5 mM $MgCl_2$, 20 mM NH_4Cl, and 50 mM K^+Hepes (pH 7) and mixed at 25 °C in a rapid quench apparatus (KinTek Instruments) with a 40 μL solution containing 10 μM [^{32}P]PEP or 10 μM [β-^{32}P]ATP, 4 mM P_i, and 50 mM K^+-Hepes (pH 7). The resulting reaction solution (80 μL) was quenched at varying conversions with 164 μL of 0.6 M HCl. Enzyme was precipitated with two 100 μL additions of CCl_4, each followed by vigorous vortexing and centrifugation for 1 min in an Eppendorf 514C microfuge. The enzyme pellet was removed, blotted dry on tissue paper, and then dissolved by boiling in 500 μL of 10 N H_2SO_4 for 1 min in a water bath. The amount of ^{32}P-labeled enzyme formed was determined by measuring the radioactivity of the resulting sample using liquid scintillation techniques. Time courses were constructed by plotting the concentration of ^{32}P-labeled enzyme formed in the reaction vs reaction time. Control reactions were carried out in which 164 μL of 0.6 M HCl was added to the enzyme solution followed by substrate. The mixture was incubated for 1 min before the enzyme was precipitated using CCl_4.

RESULTS AND DISCUSSION

Covalent Modification of PPDK with [^{32}P]-8-AzidoATP. The ATP/AMP binding site was located within the domain structure of PPDK using [α-^{32}P]-8-azidoATP to photolabel the enzyme and subtilisin Carlsberg to cut the labeled enzyme. The digests were analyzed by SDS−PAGE/autoradiography as previously described (Carroll et al., 1994). The Coomassie blue stained SDS−PAGE gel and corresponding autoradiogram obtained are shown in Figure 2. Lane 1 of the gel shows the labeled protein before treatment with subtilisin (the 96 kDa PPDK band is positioned at the top of the gel). Lane 2 shows the labeled protein following a 5 min incubation period with subtilisin. The major bands seen in lane 2 consist of protease-resistant PPDK fragments. The identities of these fragments are known from previous work (Carroll et al., 1994). The major cleavage sites on PPDK are, as illustrated in Figure 2C, at residues 227, 335, and 528. Cleavage at residue 227 generates a 25 kDa N-terminal fragment and a 67 kDa C-terminal fragment, both of which are visible in lane 2 of the Coomassie blue stained gel (Figure 2A). The 55 kDa fragment, seen as a minor band in lane 2, arises from cleavage at residue 335. Finally, the 35 kDa C-terminal fragment, which is formed by cleavage at residue 528 of the 67 and 55 kDa fragments, is clearly visible in lane 2 (the protease-sensitive remnants are not, however). The relative intensities of the 96, 67, 55, 35, and 25 kDa bands of lane 2 (Figure 2A) indicate that most of the labeled PPDK was digested within the 5 min incubation period.

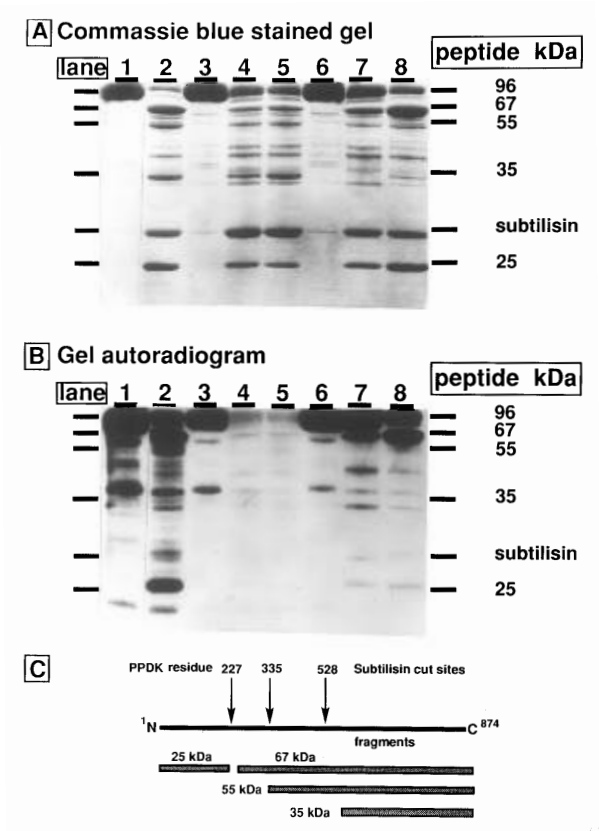

FIGURE 2: SDS−PAGE gel analysis of PPDK (10 μM) photolabeled with [α-^{32}P]-8-azidoATP (100 μM) in a solution containing 1 mM P_i, 5 mM $MgCl_2$, 10 mM NH_4Cl, 50 mM K^+Hepes (pH 7), and no inhibitor (lanes 1 and 2) or 1 mM AMPPNP (lanes 3−5) or 1 mM adenosine (lanes 6−8). Each lane contains 30 μg of unproteolyzed PPDK (lanes 1, 3, and 6) or PPDK digested with subtilisin Carlsberg for 1 min (lane 7), 5 min (lanes 2, 4, and 8), or 10 min (lane 5). The molecular masses of the PPDK fragments (kDa) and the position of subtilisin are labeled. Panels: (A) photograph of the Coomassie blue stained gel, (B) photograph of the corresponding autoradiogram, and (C) diagram of the subtilisin cut sites on the PPDK primary structure and the peptide fragments that are generated.

The intense band seen in lane 1 of the gel autoradiogram (Figure 2B) corresponds to that of the ^{32}P-labeled holoenzyme. Below this band are two minor bands (seen as very faint bands in the stained gel, Figure 2A) which correspond to unidentified contaminants. Since these two bands did not interfere with the interpretation of band patterns observed in lanes 2−8, we did not attempt to remove the contaminants.[2] Lane 2 of the gel autoradiogram reveals which of the peptide fragments (67, 55, 35, or 25 kDa) generated from the modified protein are ^{32}P-labeled. The most intense of

[2] One band migrates in between the 65 and 55 kDa bands, and the other migrates above the 35 kDa band.

the radiolabeled bands corresponds to the 96 kDa holoenzyme and to the 67 and 25 kDa peptide fragments. The 55 and 35 kDa peptide fragments do not appear to be labeled to a significant extent. These results suggest that PPDK is modified at a site between residues 1 and 226 (the 25 kDa N-terminal fragment is ^{32}P-labeled) and at a site between residues 227 and 334 (the 65 kDa fragment but not the 55 kDa fragment is ^{32}P-labeled). Because the nitrene generated upon photoexcitation of the [α-^{32}P]-8-azidoATP will indiscriminately insert into nearby protein C−H bonds, chemical modification at multiple sites is commonplace.

The photoaffinity labeling experiment was repeated in the presence of 1 mM AMPPNP, a tight binding ATP analog (K_d = 50 μM; Mehl et al., 1994), or adenosine, a weak inhibitor (K_i = 1 mM; McGuire unpublished data) of PPDK. At 1 mM AMPPNP the ATP binding site is saturated with nucleotide and hence protected from reaction with the nitrene photoadduct. In contrast, at 1 mM adenosine only a fraction of the ATP binding sites are occupied, and therefore adenosine should act primarily as a scavenger (Czarnecki et al., 1979) and UV absorption control for the AMPPNP protection experiment. The results from photolabeling in the presence of AMPPNP or adenosine are shown in lanes 3−8 of Figure 2A,B. The band corresponding to the radiolabeled holoenzyme formed in the presence of AMPPNP (lane 3) is considerably less intense than that corresponding to the PPDK photolabeled in the absence of AMPPNP (lane 1). Furthermore, lanes 4 (5 min proteolysis) and 5 (10 min proteolysis) of Figure 2B, which report the level of ^{32}P associated with the subtilisin-generated peptide fragments, are essentially clear.[3] The autoradiogram band corresponding to the 96 kDa holoenzyme labeled in the presence of adenosine (lane 6, Figure 2B) and the 67 kDa peptide fragment (lanes 7 and 8, Figure 2B) appear to be close in intensity to those determined for enzyme photolabeled in the absence of adenosine (lanes 1 and 2, Figure 2B) and significantly more intense than that determined for the enzyme photolabeled in the presence of 1 mM AMPPNP (lanes 3−5, Figure 2B). Nevertheless, some protection is provided by the adenosine as apparent from lanes 7 and 8 of the autoradiogram, in which the 25 kDa peptide band is noticeably absent. We conclude from the results described above that AMPPNP inhibits photolabeling by blocking access to the nucleotide binding site and, thus, that the photolabeling observed in the absence of the AMPPNP occurs primarily in this region.

The sites of attachment of the photoaffinity label were more precisely defined by generating small peptide fragments of the labeled protein, separating the labeled peptides, and then sequencing them. In order to minimize the technical difficulties known to be associated with using [^{32}]azidoATP as a probe (*viz.*, multiple sites of modification, low yield of radiolabeled peptide fragments, and loss of radiolabel from peptide fragments during HPLC purification; Salvucci et al., 1992), the following steps were taken. First, to maximize detection of ^{32}P-labeled peptide fragments, [γ-^{32}P]-8-azidoATP having very high specific activity was prepared (Potter & Haley, 1983) and used in place of the commercial [α-^{32}P]-8-azidoATP. Second, to minimize photolabeling at regions outside of the nucleotide binding site, PPDK was

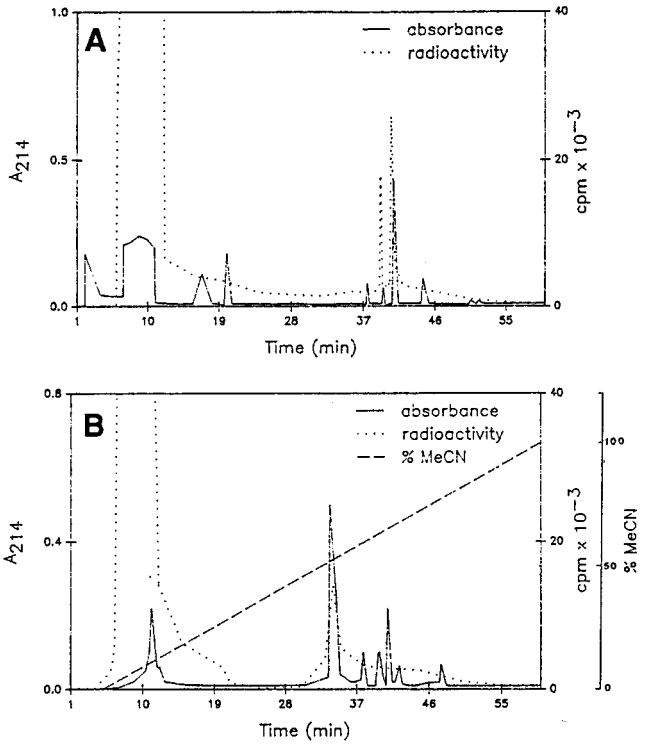

FIGURE 3: (A) Elution profile for the HPLC reversed-phase chromatographic separation of the ^{32}P-labeled peptide fraction obtained from the Al^{3+} affinity column chromatographic separation of the trypsin-digested, [γ-^{32}P]-8-azidoATP photolabeled PPDK. The column was eluted using an acetonitrile (MeCN) gradient in 0.1% TFA (see Materials and Methods for details) [—, absorbance at 214 nm; - - -, ^{32}P radioactivity (cpm)]. The first radioactive peak (eluting at 39 min) contained a single peptide which corresponded to PPDK residues 318−330 (DMQDMEFTIEEGK). The second radioactive peak (eluting at 41 min) contained two peptides having the sequences GVHFDTDLTADDLKELAEK (PPDK residues 164−182) and YLDPPLHEFVPHTEEEQAELAK (PPDK residues 618−639). (B) Same as in (A) expect that the proteolysis of the labeled PPDK was carried out with chymotrypsin in place of trypsin. The radioactive peak contained two peptides, one of which corresponded to PPDK residues 317−331 (RDMQDMEFTIEEGKL) and the other to residues 188−203 (KEAMNGEEFPQEKDQ). The single overlapping pair of peptides is 318−330 (trypsin digested) and 317−331 (chymotrypsin digested). The solvent fronts appearing at *ca.* 10 min did not contain peptide.

reacted in a 2:1 ratio with the [γ-^{32}P]-8-azidoATP (K_d *ca.* 50 μM; Figure 1 in Supporting Information). Third, for separation of the ^{32}P-labeled peptide fragments generated in the proteolytic digest, Al^{3+} affinity column chromatography (Jayaram & Haley, 1994) was carried out prior to the HPLC chromatographic separation. The affinity column binds peptides which can coordinate to the immobilized metal using phosphate (or carboxylate) substituents and thereby enriches the peptide fraction to be resolved on the HPLC column (Salvucci et al., 1992). Fourth, the photolabeled PPDK was analyzed by separately digesting two protein samples with trypsin and α-chymotrypsin and using overlapping, radioactive peptide fragments as criteria for identification of the labeling site. This approach provides an internal check as to whether the amino acid sequence of a HPLC-eluted radioactive peptide peak derives from the ^{32}P-labeled peptide.

The reversed-phase HPLC elution profiles of the tryptic and chymotryptic digests of PPDK photolabeled with [γ-^{32}P]-8-azidoATP are shown in panels A and B of Figure 3, respectively. In both chromatographies a majority of the radiolabel, lost from the carrier peptide, eluted from the HPLC column in the (peptide-free) solvent front. The two

[3] Bound AMPPNP retards the rate of subtilisin-catalyzed proteolysis (Carroll et al., 1994), and for this reason the amount of subtilisin used in the digestion was increased as was the final incubation period.

radioactive peptide peaks (at 39 and 41 min) observed in the chromatography of the tryptic digest were subjected to automated peptide sequencing. The first peak consisted of a single peptide, DMQDMEFTIEEGK, corresponding to residues 318−330 in PPDK. The second peak consisted of two peptides, GVHFDTDLTADDLKELAEK and YLDPPLHEFVPHTEEEQAELAK, corresponding to PPDK residues 164−182 and 618−639, respectively. The HPLC elution profile of the chymotryptic digest (Figure 3B) shows a single radioactive peptide peak. Sequence analysis identified two peptides having the sequences KEAMNGEEFPQEKDQ (residues 188−203 in PPDK) and RDMQDMEFTIEEGKL (residues 317−331 in PPDK). The tryptic peptides 164−182 and 618−639 and chymotryptic peptide 188−203 do not overlap with one another and therefore cannot be considered as components of the nucleotide binding site. However, the 317−331 peptide from the chymotrypsin digest overlaps with the 318−330 peptide of the trypsin digest, and thus, we are confident that this segment of sequence contributes to the nucleotide binding site. In Figure 4A, the overall fold of the PPDK N-terminal domain is shown highlighting residues 320−327, a β-strand, in red. The strand occurs in one of two β-sheets forming a crevice at the subdomain interface. The results from site-directed mutagenesis experiments and structural analyses (see below) provide additional evidence for the location of the nucleotide binding site within this crevice.

Site-Directed Mutagenesis of Invariant Residues within the N-Terminal Domain of PPDK. The object of this study is the identification of amino acid residues, within the N-terminal domain of PPDK, essential to nucleotide binding/catalysis. The residues that were replaced by site-directed mutagenesis were selected from among clusters of invariant residues identified by alignment of the four known PPDK sequences [*C. symbiosum* (Pocalyko et al., 1990), *Zea mays* (Matsuoka et al., 1988), *Entomoeba histolytica* (Bruchaus & Tannich, 1993), and *Flaveria trinervia* (Roche & Westhoff, 1990).[4] The first two residues targeted for replacement, G248 and G254, wrere selected from a highly conserved, polar, glycine-rich motif, ^{245}GNKGETSGTG^{254}. The Gly residues were replaced with Ile and the catalytic properties of the mutant enzymes measured and compared to those of wild-type PPDK. Assuming that the Gly residues were conserved for steric reasons, the large side chain of the Ile residue would be expected to significantly alter local structure. If the altered region is associated with the nucleotide binding site, substrate binding/catalysis would be impaired.

The yield and specific activities of the G248I and G254I mutants are listed in Table 1. Both mutants were expressed and purified in high yield, and both mutants appeared, on the basis of their stability toward proteolysis and retention of activity upon prolonged storage at 4 °C, to be as stable as wild-type PPDK. The specific activity of the G248I mutant was found to be lower than that of wild-type PPDK but only by a factor of 6. On the other hand, the specific activity of the G254I mutant is 1000-fold lower than that of wild-type PPDK. Our attention focused on determining which step(s) of the reaction catalyzed by the G254I mutant is (are) impaired. Initial velocity techniques were used to measure steady-state kinetic constants for the forward and reverse directions of the full reaction (Table 2), and transient kinetic techniques were used to measure the single turnover rates for catalysis of the two partial reactions (E·ATP·P_i → E−PP·AMP·P_i → E−P·AMP·PP_i and E·PEP → E−P·pyruvate) (Figures 5A and 6A). The k_{cat} for catalysis in the ATP-forming direction is *ca.* 300-fold lower in the mutant, and the k_{cat} measured in the AMP-forming direction is *ca.* 3000-fold lower (Table 2). The K_m values measured for AMP, PP_i, and PEP as substrates for wild-type PPDK and

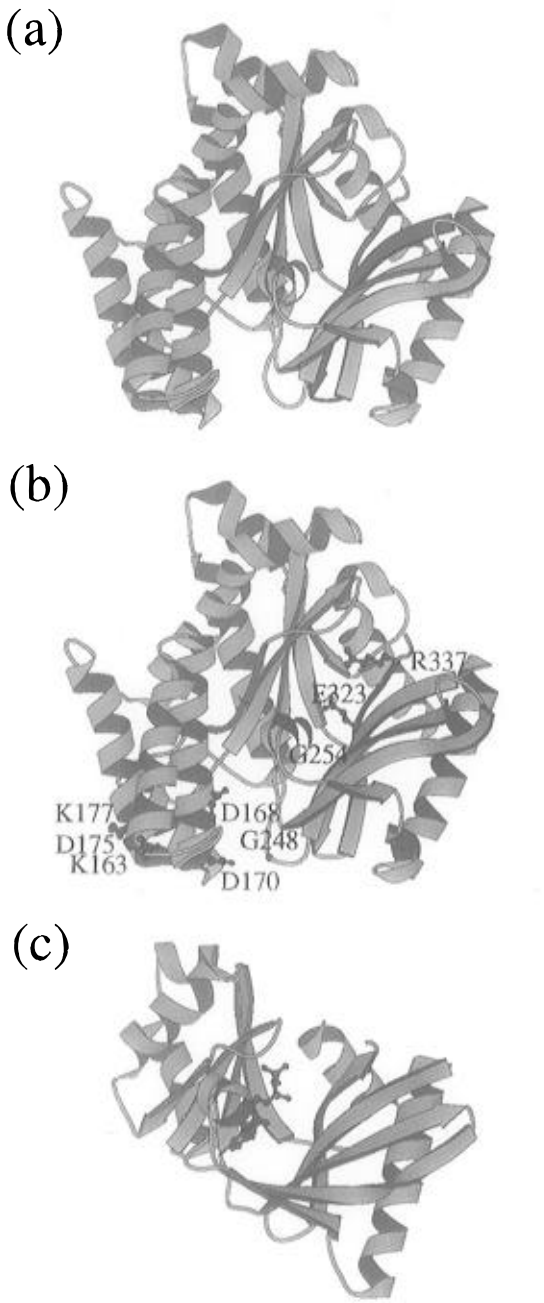

FIGURE 4: (a) The overall fold of the N-terminal domain of *C. symbiosum* PPDK highlighting the site of modification by the photoaffinity label 8-azidoATP in red. (b) The overall fold of the N-terminal domain of *C. symbiosum* PPDK highlighting the three subdomains in green, pink, and lavender. The side chains of the amino acid residues replaced by site-directed mutagenesis are shown in red, and the specific amino acids replaced in the site-directed mutants are listed in Table 2. (c) The overall fold of the nucleotide binding domains of D-Ala-D-Ala ligase highlighting the subdomains in green and lavender according to their similarity to the subdomains of the PPDK N-terminal domain. The bound ADP is shown in red.

[4] As pointed out in a previous report on the *C. symbiosum* PPDK sequence (Pocalyko et al., 1990), the stretch of sequence comprising the N-terminal domain (1−340) does not contain a recognizable nucleotide binding/P-loop motif.

Table 1: Yields and Specific Activities of Purified PPDK Mutants[a]

PPDK	yield (mg/g of cell)	specific activity (unit/mg)[b]
wild type	20	24
*Bg1*II	23	20
K163L	11	33
D168A	18	7
D170A	15	25
D175A	13	12
K177L	6	15
G248I	10	3.8
G254I	10	0.03
E323L	8	none
R337L	9	0.40

[a] See Materials and Methods for details. [b] The assay solutions used for the measurement of the specific activity contained 0.5 mM PEP, 0.5 mM AMP, 1 mM PP_i, 5 mM $MgCl_2$, 40 mM NH_4Cl, 22 units/mL lactate dehydrogenase, and 0.2 mM NADH in 20 mM imidazole hydrochloride (pH 6.4) at 25 °C.

Table 2: Steady-State Kinetic Constants for Wild-Type PPDK, G254I PPDK, and R337L PPDK Catalysis

Catalysis of AMP + PP_i + PEP → ATP + P_i + Pyruvate PPDK[a]	K_m (mM)	k_{cat} (s^{-1})[g]
wild type (0.016 μM)		
vary AMP[b]	0.007 ± 0.0005	26
vary PP_i[c]	0.07 ± 0.01	30
vary PEP[d]	0.027 ± 0.0005	36
G254I (14 μM)		
vary AMP[b]	1.3 ± 0.1	0.09
vary PP_i[c]	1.2 ± 0.2	0.12
vary PEP[d]	0.012 ± 0.009	0.04
R337L (0.14 μM)		
vary AMP[e]	0.085 ± 0.007	1.1
vary PP_i[c]	3.7 ± 0.2	2.6
vary PEP[d]	0.006 ± 0.0004	1.0

Catalysis of ATP + P_i + Pyruvate → AMP + PP_i + PEP PPDK[f]	k_{cat} (s^{-1})[g]
wild type (1 μM)	5.4
G254I (40 μM)	0.002
R337L (20 μM)	0.035

[a] Reactions contained 5 mM $MgCl_2$ and 40 mM NH_4Cl in 20 mM imidazole hydrochloride (pH 6.8, 25 °C). [b] Reactions contained 2.5 mM PP_i and 0.5 mM PEP. [c] Reactions contained 0.5 mM AMP and 0.5 mM PEP. [d] Reactions contained 1.0 mM PP_i and 0.5 mM AMP. [e] Reactions contained 2.5 mM PP_i and 0.5 mM PEP. [f] Reactions contained 2 mM [^{14}C]ATP, 5 mM pyruvate, 5 mM P_i, 20 units of inorganic pyrophosphatase, 5 mM $MgCl_2$, and 10 mM NH_4Cl in 50 mM K^+Hepes (pH 7.0, 25 °C). [g] These values are defined within 10−20% error.

the G254I mutant (Table 2) indicate which segments of the overall reaction have been altered in the mutant. Specifically, the K_m values for AMP and PP_i are increased by a factor of 100 and 10, respectively, while the K_m value for PEP is not increased. These results suggested that the nucleotide partial reaction and not the pyruvate partial reaction is inhibited in the mutant.

The transient kinetic measurements of the partial reactions confirmed this deduction. The time courses measured for a single turnover of [β-^{32}P]ATP and P_i catalyzed by wild-type PPDK and G254I PPDK (Figure 5A) show that the level of E−PP·AMP·P_i and E−P·AMP·PP_i formed by the mutant (measured by the amount of ^{32}P-labeled enzyme isolated from the quenched reaction) is negligible compared to that formed by wild-type PPDK. In contrast, the time courses for the single turnovers of [^{32}P]PEP (to form ^{32}P-labeled E−P) catalyzed by wild-type PPDK and G254I PPDK are essentially identical (Figure 6A). G254 thus appears to affect catalysis at the nucleotide active site but not catalysis at the

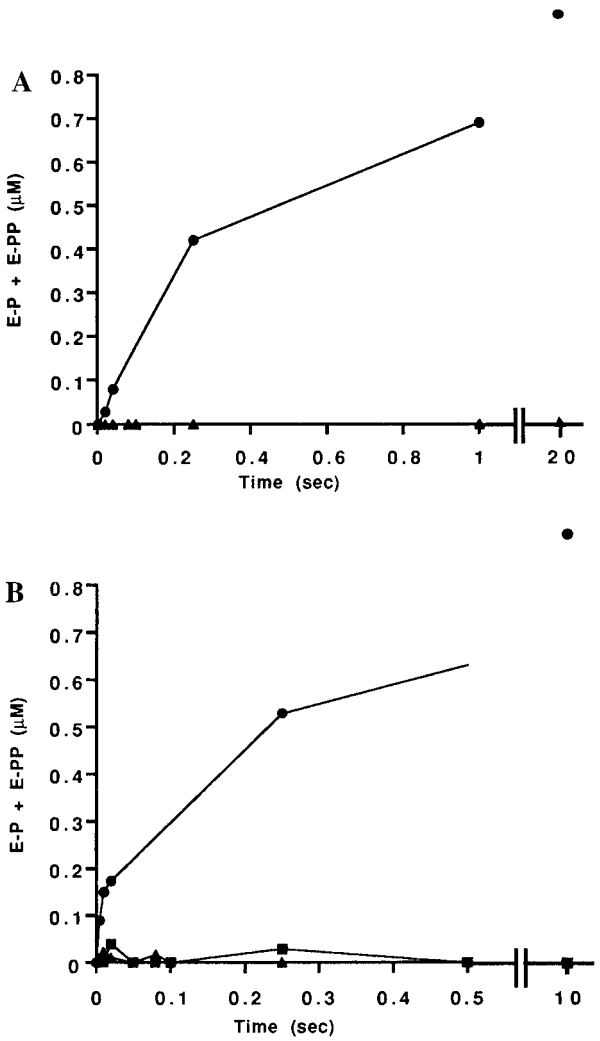

FIGURE 5: Time course of the formation of phosphoryl enzyme intermediates in the nucleotide half-reaction of wild-type PPDK (circles) and (A) G254I PPDK (triangles) or (B) E232L PPDK (triangles) and R337L PPDK (squares). For each time point, a 40 μL solution containing 80 μM enzyme active sites, 5 mM $MgCl_2$, 20 mM NH_4Cl, and 50 mM K^+Hepes (pH 7.0) was mixed with an equal volume solution containing 10 μM [β-^{32}P]ATP, 4 mM P_i, and 50 mM K^+Hepes (pH 7). Final concentrations of each species after mixing were as follows: 40 μM enzyme, 5 μM [β-^{32}P]ATP, 2 mM P_i, 2.5 mM $MgCl_2$, 10 mM NH_4Cl, and 50 mM K^+Hepes (pH 7).

pyruvate site. As is shown in Figure 4B and described in the following section, G254 is located on a β-strand contained within one of the two β-sheets in the nucleotide binding domain while G248 is located on a connecting loop.

Other invariant amino acid residues (Asp168, Asp170, and Asp175; Lys163 and Lys177) that were replaced on the basis of the sequence alignment were found to have little or no apparent role in substrate binding/catalysis. As shown in Table 1, the specific activities of the mutant enzymes are within a factor of 3 of that of wild-type PPDK. We now know, as is illustrated Figure 4B, that the mutated residues occupy solvent-exposed sites on the protein that are remote from the crevice formed by the β-sheets.

The preparation of the last two mutants, E323L and R337L PPDK, followed the determination of the enzyme crystal structure (Herzberg et al., 1996). As shown in Figure 4B the charged side chains of E323 and R337 project into the crevice formed by the two β-sheet structures of the N-terminal domain. If the nucleotide active site is located here, replacement of these residues with Leu would affect substrate

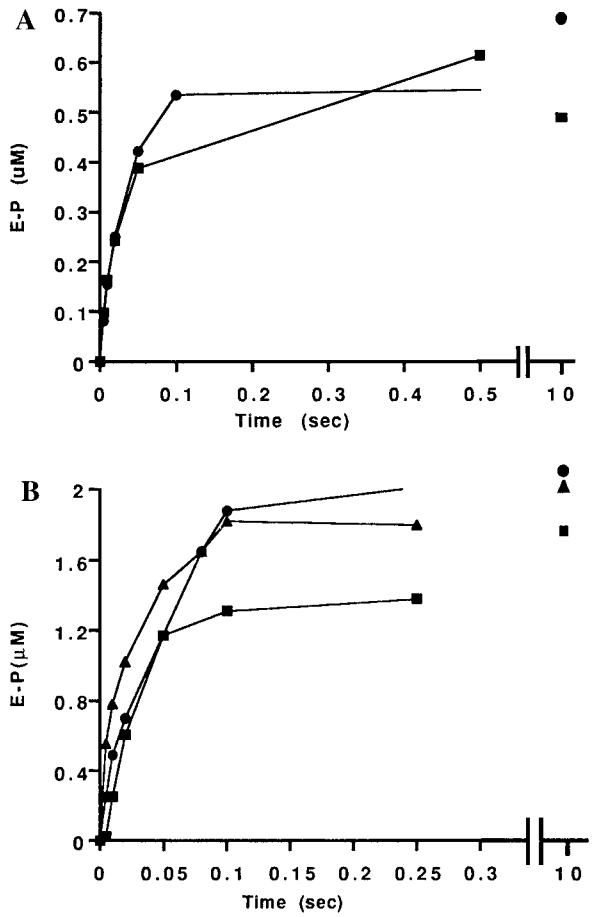

FIGURE 6: Time course of the formation of phosphoryl enzyme intermediates in the PEP half-reaction of wild-type PPDK (circles) and (A) G254I PPDK (squares) or (B) E323L PPDK (triangles) and R337L PPDK (squares). For each time point, a 40 μL solution containing 80 μM enzyme active sites, 5 mM $MgCl_2$, 20 mM NH_4-Cl, and 50 mM K^+HEPES (pH 7) was mixed with an equal volume solution containing 10 μM [^{32}P]PEP and 50 mM K^+Hepes (pH 7.0). Final concentrations of each species after mixing were as follows: 40 μM enzyme, 5 μM [^{32}P]PEP, 2.5 mM $MgCl_2$, 10 mM NH_4Cl, and 50 mM K^+Hepes (pH 7).

binding/catalysis. The two mutants were expressed and purified in high yield (Table 1). The specific activity of the E323L mutant is lower than our detection level (<0.0001 unit/mg)[5] while that of the R337L mutant is *ca*. 60-fold lower than that of wild-type PPDK (Table 1). The R337 PPDK was sufficiently active to measure the steady-state rate constants for catalysis of the full reaction; however, the E323L PPDK was not. The k_{cat} value for R337L PPDK catalysis in the ATP-forming direction is *ca*. 10-fold smaller than that of wild-type PPDK, and the k_{cat} value for catalysis in the AMP-forming direction is *ca*. 100-fold smaller (Table 2). The K_m value for AMP as a substrate for R337L PPDK is *ca*. 10-fold larger than that measured with wild-type PPDK, the K_m value for PP_i is *ca*. 50-fold larger, and the K_m value for PEP is *ca*. 4-fold smaller. As was observed with the G254I mutant, catalysis of the nucleotide partial reaction appears to be selectively inhibited.

R337L and E323L PPDK catalysis of the nucleotide and pyruvate partial reactions was examined using the transient kinetic methods described above. The time courses measured for a single turnover of [β-^{32}P]ATP and P_i catalyzed by wild-type and R337L and E323L PPDK (Figure 5B) show that the level of E−PP·AMP·P_i and E−P·AMP·PP_i formed by the mutants is negligible compared with that formed by wild-type PPDK. In contrast, the time courses for the single turnovers of [^{32}P]PEP catalyzed by wild-type PPDK and the two mutants are essentially identical (Figure 6B). R337 and E323 thus appear to play important roles in catalysis at the nucleotide active site but not in catalysis at the pyruvate site.

Assignment of the Nucleotide Binding Site Based on Structural Similarity to a Class of ATP/ADP Utilizing Enzymes. The N-terminal domain consists of three subdomains (Herzberg et al., 1996). One of these spans residues 2−111 and 199−249 and has an $\alpha+\beta$-fold that includes a five-stranded antiparallel β-sheet (colored green in Figure 4B). The second subdomain (residues 112−198) forms a four-helix bundle that is inserted into the first subdomain (colored pink in Figure 4B). The third subdomain (residues 250−340) adopts an $\alpha+\beta$-fold in which a single helix packs against a five-stranded antiparallel β-sheet (colored lavender in Figure 4B). Despite the lack of significant sequence identity, the fold of the first and third subdomains is similar to that of the nucleotide binding domains of several ATP/ADP converting enzymes of known structure: D-Ala-D-Ala ligase (Fan et al., 1994, 1995) and succinyl-CoA synthetase and glutathione synthetase (Wolodko et al., 1994; Yamaguchi et al., 1993). These enzymes belong to a distinct class of nucleotide binding enzymes which lack the typical Rossman fold (Rossmann et al., 1874) or P-loop motif (Saraste et al., 1990) found in many other nucleotide binding enzymes.

The α-carbon atoms of the PPDK N-terminal domain were superimposed on the nucleotide domains of D-Ala-D-Ala ligase (Fan et al., 1994), succinyl-CoA synthetase (Wolodko et al., 1994), and glutathione synthetase (Yamaguchi et al., 1993) to arrive at rms deviations of 2.2 Å for 155 residue pairs, 2.4 Å for 155 residue pairs, and 2.4 Å for 126 residue pairs, respectively (Herzberg et al., 1996). The nucleotide binding domain of D-Ala-D-Ala ligase, together with bound ADP, is shown in Figure 4C in the same orientation as that of the PPDK domain. Indeed, the ADP binds in the interface between the two β-sheets. In that structure (determined in complex with Mg^{2+}/ADP/phosphinophosphate inhibitor) a Lys residue (K215), located on a large ω-loop that flanks the crevice, interacts with the β-phosphate group of ADP (Fan et al., 1994, 1995; Shi & Walsh, 1994). In the PPDK structure, the catalytic His455 (of the central domain) must occupy the site near the nucleotide β-phosphate.[6] Thus, assuming that the orientation of the bound nucleotide is similar in both proteins, the adenosine moiety would be covered by the ω-loop while the tripolyphosphate moiety would be accessible to His455.

The location of the nucleotide binding site at the interface of PPDK N-terminal subdomains 1 and 3 is substantiated by the location of the site modified by the photoaffinity label (8-azidoATP) (Figure 4A) and by the catalytic properties of the site-directed mutants listed in Table 1. K163, D168, D170, D175, and K177 are solvent-exposed residues that are remote from the proposed nucleotide binding site (Figure 4B). Thus, the replacement of these residues does not significantly alter the catalytic activity. Ile substitution of G248, located on a solvated loop connecting subdomains 1

[5] The specific activity of the E323D PPDK mutant is also below detection limits (McGuire, unpublished data).

[6] Activated His455 requires a change in its side-chain conformation compared with that observed in the crystal structure (Herzberg et al., 1996).

and 3, caused a small but noticeable decrease in the specific activity of the enzyme. In contrast, Ile replacement of G254, which is located near the bottom of the crevice formed between the two β-sheets, resulted in a substantial drop in catalysis at the nucleotide active site. Modeling shows that the Ile side chain would project into the core of subdomain 3, where the available space can accommodate only the α-carbon hydrogen atom of a glycine. The large impact on catalysis would result from changes in fold necessary to accommodate the large Ile side chain. Finally, E323 and R337 are both located in the crevice and are likely to be directly involved in Mg(II) and ATP/P_i binding, respectively (Herzberg et al., 1996).

Conclusions. PPDK folds into three consecutive domains: N-terminal, central, and C-terminal. Previous studies have shown that the active site which catalyzes the pyruvate partial reaction is located on the C-terminal domain while the catalytic histidine residue (His455) resides on the central domain. The present studies show that the ATP/AMP binding site is located at the PPDK N-terminal domain. The ATP is proposed to bind in a crevice formed at the interface of subdomains 1 and 3 in analogy to the ADP binding to the D-Ala-D-Ala ligase. The adenine ring binds at the bottom underneath on ω-loop, and the tripolyphosphate moiety is oriented toward the solvent such that it is accessible to His455. Modeling shows that the Mg^{2+} cofactor and the P_i cosubstrate can also bind to the crevice, close to the β-P of the ATP (Herzberg et al., 1996). During the course of catalytic turnover the central domain must move from the N-terminal domain, where His455 is phosphorylated, to the C-terminal domain where the phosphoryl group is transferred from the phosphohistidine to pyruvate. The movement of the central domain between the two substrate binding sites displaces His455 by *ca*. 45 Å and has been modeled as a "swivel" motion around the two linker peptides that connect the central domain to the nucleotide and pyruvate domains (Herzberg et al., 1996).

SUPPORTING INFORMATION AVAILABLE

One table giving specifications on PCR-generated PPDK site-directed mutants and one figure showing saturation curves for [γ-^{32}P]-8-azidoATP photolabeling of PPDK and for ATP protection against [γ-^{32}P]-8-azidoATP photolabeling of PPDK (3 pages). Ordering information is given on any current masthead page.

REFERENCES

Bracchus, I., & Tannich, E. (1993) *Mol. Biochem. Parasitol. 62*, 153.

Carroll, L. J., Mehl, A. F., & Dunaway-Mariano, D. (1989) *J. Am. Chem. Soc. 111*, 5965.

Carroll, L. J., Dunaway-Mariano, D., Saith, S. M., & Chollet, R. (1990) *FEBS Lett. 274*, 178.

Carroll, L. J., Xu, Y., Thrall, S. H., Martin, B. M., & Dunaway-Mariano, D. (1994) *Biochemistry 33*, 1134.

Chang, A. C. Y., & Cohen, S. (1978) *J. Bacteriol. 134*, 1141.

Cleland, W. W. (1979) *Methods Enzymol. 63*, 103.

Cooper, A. G., & Kornberg, H. L. (1974) in *The Enzymes* (Boyer, P. D., Ed.) 3rd ed., p 631, Academic Press, New York.

Czarnecki, J., Geahlen, R., & Haley, B. E. (1979) *Methods Enzymol. 56*, 642.

Erlich, H. A., Ed. (1992) *PCR Technology Principles and Applications for DNA Amplification*, W. H. Freeman and Co., New York.

Fan, C., Maws, P. C., Walsh, C. T., & Knox, J. R. (1994) *Science 266*, 439.

Fan, C., Moews, P. C., Shi, Y., Walsh, C. T., & Know, J. R. (1995) *Proc. Natl. Acad. Sci. U.S.A. 92*, 1172.

Herzberg, O., Chen, C. C. H., Kapadia, G., McGuire, M., Carroll, L. J., Noh, S. J., & Dunaway-Mariano, D. (1996) *Proc. Natl. Acad. Sci. U.S.A. 93*, 2652.

Jayaram, B., & Haley, B. (1994) *J. Biol. Chem. 269*, 3233.

Matsuoka, M., Ozeki, Y., Yamamoto, N., Hirano, H., Kano-Murakami, Y., & Tanaka, Y. (1988) *J. Biol. Chem. 263*, 11080.

Mehl, A. F., Xu, Y., & Dunaway-Mariano, D. (1994) *Biochemistry 33*, 1093.

Pocalyko, D. J., Carroll, L. J., Martin, B. M., Babbitt, P. C., & Dunaway-Mariano, D. (1990) *Biochemistry 29*, 10757.

Potter, R. L., & Haley, B. E. (1983) *Methods Enzymol. 91*, 613.

Reeves, R. E., Menzies, R. A., & Hsu, D. S. (1968) *J. Biol. Chem. 243*, 5486.

Rosche, E., & Westhoff, P. (1990) *FEBS Lett. 273*, 116.

Rossman, M. G., Moras, D., & Olsen, K. W. (1974) *Nature (London) 250*, 194.

Salvucci, M. E., Chavan, A. J., & Haley, B. E. (1992) *Biochemistry 31*, 4479.

Sambrook, J., Fritsch, E. F., & Maniatis, T. (1989) *Molecular Cloning*, 2nd ed., Cold Spring Harbor Press, New York.

Sanger, F., Miklen, S., & Coulson, A. R. (1977) *Proc. Natl. Acad. Sci. U.S.A. 74*, 5463.

Saraste, M., Sibbald, P. R., & Wittinghofer, A. (1990) *Trends Biochem. Sci. 15*, 430.

Shi, Y., & Walsh, C. T. (1995) *Biochemistry 34*, 2768.

Spronk, A. M., Yoshida, H., & Wood, H. G. (1976) *Proc. Natl. Acad. Sci. U.S.A. 73*, 4415.

Stone, K. L., Lopresti, M. B., Maron, C. J., DeAngelis, R., & Williams, K. R. (1989) in *Practical Guide to Protein and Peptide Purification for Microsequencing* (Matsudaira, P. T., Ed.) Academic Press, San Diego, CA.

Thrall, S. H. (1993) Ph.D. Dissertation, University of Maryland, College Park, MD.

Thrall, S. H., & Dunaway-Mariano, D. (1994) *Biochemistry 33*, 1103.

Thrall, S. H., Mehl, A. F., Carroll, L. J., & Dunaway-Mariano, D. (1993) *Biochemistry 32*, 1803.

Wang, H. C., Ciskanik, L., Dunaway-Mariano, D., von der Saal, W., & Villafranca, J. J. (1988) *Biochemistry 27*, 625.

Wolodko, W. T., Fraser, M. E., James, M. N. G., & Bridger, W. A. (1994) *J. Biol. Chem. 269*, 10883.

Wood, H. G., O'Brien, W. E., & Michaels, G. (1977) *Adv. Enzymol. Relat. Areas Mol. Biol. 45*, 85.

Xu, Y., McGuire, M., Dunaway-Mariano, D., & Martin, B. (1995a) *Biochemistry 34*, 2195.

Xu, Y., Yankie, L., Shen, L., Jung, Y.-S., Mariano, P. S., Dunaway-Mariano, D., & Martin, B. (1995b) *Biochemistry 34*, 2181.

Yamaguchi, H., Kato, H., Hata, Y., Takaaki, N., Kimura, A., Oda, J., & Katsube, Y. (1993) *J. Mol. Biol. 229*, 1083.

Yankie, L., Yuan, X., & Dunaway-Mariano, D. (1995) *Biochemistry 34*, 2188.

BI960275K